Investigation of size and electronic effects on Kapitza conductance with non-equilibrium molecular dynamics

R. E. Jones, J. C. Duda, X. W. Zhou, C. J. Kimmer, and P. E. Hopkins

Citation: Appl. Phys. Lett. **102**, 183119 (2013); doi: 10.1063/1.4804677
View online: http://dx.doi.org/10.1063/1.4804677
View Table of Contents: http://apl.aip.org/resource/1/APPLAB/v102/i18
Published by the American Institute of Physics.

Investigation of size and electronic effects on Kapitza conductance with non-equilibrium molecular dynamics

R. E. Jones,[1,a)] J. C. Duda,[2] X. W. Zhou,[1] C. J. Kimmer,[3] and P. E. Hopkins[2]
[1]*Department of Mechanics of Materials, Sandia National Laboratories, Livermore, California 94550, USA*
[2]*Department of Mechanical and Aerospace Engineering, University of Virginia, Charlottesville, Virginia 22904, USA*
[3]*School of Natural Sciences, Indiana University Southeast, New Albany, Indiana 47150, USA*

(Received 4 March 2013; accepted 28 April 2013; published online 10 May 2013)

In nanosystems, the thermal resistance between materials typically dominates the overall resistance. While size effects on thermal conductivity are well documented, size effects on thermal boundary conductance have only been speculated. In response, we characterize the relationship between interfacial resistance and material dimension using molecular dynamics. We find that the interfacial resistance increases linearly with inverse system length but is insensitive to cross-sectional area. Also, from the temperature-dependence of interfacial resistance, we conclude that contributions of short-wavelength phonons dominate. Lastly, by coupling the molecular dynamics to a two-temperature model, we show that electron-mediated transport has little effect on thermal resistance. © *2013 AIP Publishing LLC*. [http://dx.doi.org/10.1063/1.4804677]

It is well-known that when heat passes through an interface between two different materials, the temperature across the interface exhibits an abrupt change,[1,2] and the overall resistivity increases. To illustrate this, consider a heat flux J passing through two materials A and B in series with lengths L_A and L_B and thermal conductivities κ_A and κ_B, respectively. The total temperature change ΔT across both materials is $\Delta T = JL_A/\kappa_A + [\![T]\!] + JL_B/\kappa_B$, where $[\![T]\!]$ is the temperature jump at the A:B interface. The overall apparent system thermal resistivity $\Sigma \equiv \frac{\Delta T}{J(L_A+L_B)}$ is

$$\Sigma = \frac{L_A/\kappa_A}{L_A+L_B} + \frac{\sigma}{L_A+L_B} + \frac{L_B/\kappa_B}{L_A+L_B}, \tag{1}$$

where $\sigma \equiv [\![T]\!]/J$ is the Kapitza resistance ($h \equiv 1/\sigma$ is the Kapitza conductance). Equation (1) indicates that the overall system resistivity is a sum of the length-weighted average of the resistivity of the two materials plus the Kapitza resistance σ averaged over the total system length $L \equiv L_A + L_B$. Typical values of h at solid-solid interfaces range from 10 to 500 MW/m^2 K at room temperature.[3–6] So at the nanoscale, say $L_A + L_B \approx 100$ nm, the interfacial resistivity $\sigma/(L_A + L_B)$ can reach 0.02-1 m K/W and dominate the overall thermal resistance. This phenomenon can be utilized to increase the figure-of-merit in thermoelectric applications;[7,8] it can also cause local heating leading to catastrophic failure in microelectronic devices.[9]

Unlike at interfaces between bulk materials, Kapitza resistance has been speculated to be size-dependent at the nanoscale,[10–12] although this sensitivity has not been well established. Understanding the effect of system size is important to design optimal nanostructured thermoelectric materials and effective thermal management of contacts to nanoscale devices. Molecular dynamics (MD) provides a means to study thermal boundary resistance[13–19] where phonons are thought to dominate interfacial thermal resistance in both metal-semiconductor or semiconductor-semiconductor interfaces;[5] however, the range of computationally feasible dimensions is limited by the cost of thermal transport studies where relatively long times are needed for converged results.

Effects of system length $L \equiv L_A + L_B$ on Kapitza resistance σ have been explored previously using MD simulations;[10,12,20–22] however, controversy exists among these studies. For instance, the contact resistance of networks of single walled carbon nanotubes was found to increase linearly with the inverse of tube length by Evans *et al.*[20] where the tubes were preferentially aligned perpendicular to the primary heat flux direction, but no such a length dependence was discovered by Carlborg *et al.*[21] where the tubes were parallel and embedded in an Ar matrix. Merabia and Termentzidis[22] demonstrated that the thermal boundary resistance of a Lennard-Jones (LJ) bicrystal increases with $L^{-3/2}$, although the data fits L^{-1} equally well. Clearly, the effect of system size on σ is complex, and σ can depend on many other factors such as geometry, materials, and temperature. Furthermore, ignoring the contributions of electrons in metal-semiconductor systems could exacerbate size-effects since the distribution of phonon mean-free-paths can be much wider than that of the electron system.[23,24]

In this paper, we perform systematic MD simulations of thermal transport across a metal/semiconductor interface using the "direct method"[13–19] with systems more than 0.17 μm long to gain a fuller picture of the size-scaling effect. The dimension of the cross-section perpendicular to the heat flux direction, the length-scale along the heat flux direction, and the relative length ratio of the materials comprising the bicrystal are explored separately. In addition, to distinguish this effort from previous work, we (a) significantly expand the time scale used in the previous MD simulations[13–19,22] from a few ns to more than 100 ns to establish reliable trends; (b) use both a Stillinger-Weber (SW) potential to explore a realistic Al:GaN interface and a simpler Lennard-Jones potential to facilitate the understanding of the phenomenon; and (c) enhance the SW Al:GaN with a two-temperature model

a)Electronic mail: rjones@sandia.gov

(TTM) to examine electron-mediated effects on thermal boundary resistance.[25]

Many of our previous MD simulations on thermal transport[26–28] have employed a GaN SW potential[29] parameterized by Béré and Serra.[30,31] We developed an Al-Ga-N interatomic potential given the constraint that the GaN SW potential[30,31] remained unchanged (see Zhou *et al.*[32] for details). The Al:GaN bicrystal was initially constructed with lattice constants: $a_{Al} = 4.05$ Å for the FCC Al and $a_{GaN} = 3.19$ Å and $c_{GaN} = 5.20$ Å for the wurtzite GaN. The {111} Al plane and {0001} GaN plane are normal to the heat flux direction with Al in contact with Ga. The lateral boundaries are periodic such that {112} Al shares a boundary with $\{\bar{1}110\}$ GaN and {220} Al shares a boundary with $\{11\bar{2}0\}$, as in Ref. 32. Cold, fixed boundary atoms cap the system in the flux direction. Given the intrinsic lattice mismatch in the Al:GaN bicrystal and a potentially difficult thermalization, the careful mechanical and thermal equilibration procedures, outlined in Zhou *et al.*,[26–28] were followed. The resulting system had low lattice mismatch strains of 0.001 in the $\langle 112 \rangle$ Al direction and -0.003 in the $\langle 220 \rangle$ Al direction with virtually no rearrangement at the interface and no defect structures generated.

The LJ system was constructed similarly,[33] with the {100} plane of the LJ bicrystal perpendicular to the heat flux direction. The LJ potential was parameterized for Ar.[34] The two crystals differ from one another only in their atomic mass (40 and 120 amu, respectively), so that no lattice strain was induced.

Once the systems were relaxed and thermalized, equal and opposite heat fluxes were applied to "hot" and "cold" regions as in the usual application of the "direct" method of measuring thermal conductivity.[28,35,36] The energy flux was effected by controlling the input of kinetic energy over time.[37–40] This flux-control scheme, together with Verlet dynamics, maintained a constant system energy throughout the data collection phase. In preliminary runs, the flux, J, was adjusted so that the maximum temperature jump was <30 K in the Al:GaN system and <3 K in the LJ system to remain as close to the linear regime as the inherent thermal noise will allow. This resulted in $J = 0.12$–0.2 meV/ps Å^2 for the Al:GaN systems and 0.0035 meV/ps Å^2 for the LJ system. For each study multiple samples were made in order to estimate statistical errors, e.g., 110 ns of total run-time for the smaller Al:GaN systems, 72 ns for the larger ones, and >25 ns for all LJ runs.

For the SW simulations which modeled the additional heat-flux mediated by a free electron gas in the Al, a finite element implementation of the TTM[41] was coupled to the lattice with a temperature-field based thermostat.[42] The TTM was applied in the metal except for the flux control region where the dynamics follow the energy flux constraint. At the edge of the Al flux control region and the Al:GaN interface the electron temperature was given insulating boundary conditions. The insulating boundary conditions are consistent with a thermal pathway from the metal electrons to the semiconductor's phonons being through the metal's phonons. The electron-phonon (e-ph) coupling was also extended into the GaN near the interface to test the hypothesis of direct metal electron-semiconductor phonon coupling.[43,44] The additional parameters required by the TTM are the Al electron heat capacity: 40.5 kJ/K m^3 at 300 K and 121.5 kJ/K m^3 at 1000 K (using a Sommerfeld parameter of 135 J/K^2 m^3); the Al electron thermal conductivity: 256.5 W/m K at 300 K and 769.5 W/m K at 1000 K (calculated using the Wiedemann-Franz-Lorentz relation); and the e-ph coupling coefficient: 0.245 W/K μm^3 (which is assumed constant[45]).

Two material systems were investigated: LJ with an acoustic mismatch; and Al-GaN, with and without TTM coupling. In all cases the typical temperature profile has a temperature jump over a few Å at the interface and relatively small temperature changes within both regions of the bicrystal (English *et al.*[46] and Zhou *et al.*[32] has typical temperature profiles for the LJ and SW systems, respectively).

As a preliminary study, the sensitivity of the interface resistance to the width of the system was investigated with the Al:GaN system. For system of length $\approx$174 Å ($n_{Al} = 10$ uc (unit cells)), $n_{GaN} = 20$ uc, 3 different cross-sections were studied: (a) Al 29×10 uc^2 and GaN 26×9 uc^2 ($\approx 144 \times 29$ Å^2), (b) Al 58×10 uc^2 and GaN 52×9 uc^2 ($\approx 288 \times 29$ Å^2), and (c) Al 29×20 uc^2 and GaN 26×18 uc^2 ($\approx 144 \times 58$ Å^2), which have the same small mismatch strain as in the rest of the Al:GaN systems. The same Kapitza conductance, 0.075 GW/m^2 K, was obtained to within an estimated error of ± 0.0002 GW/m^2 K, convincingly indicating that the conductance is not sensitive to lateral dimensions.

Using the same Al:GaN system, the data shown in Fig. 1(a) indicate a linear relationship between phonon-mediated interface resistance σ and inverse total length $1/L$ of the bicrystal at both 300 K and 1000 K. At 300 K, all the data points obtained for two values of n_{Al}/n_{GaN} at shorter system lengths, $L \leq 500$ Å, are close to the trend lines. The data points for the longer systems (2:1) fall slightly below the trend; however, the values for the longest systems revert to the linear trend in a manner that is suggestive of a length-insensitive bulk value that is approximately equal to the linear extrapolation of the bulk limit, $\sigma \approx 4.73$ m^{2}K/GW. Similar behavior was observed in bulk resistivity[12,47,48] (see Ref. 48 for a thorough discussion). This linear trend is significant since it appears to be another instance of the Matthiessen scattering rule, analogous to the thermal resistivity of an interface-free material in contact with heat baths being linearly related to the inverse of the system length, which is widely cited and employed.[12,26,47–50] Also, it is clear that size effects are less prominent at higher temperatures, where the phonon mean-free-paths are shorter; and, as Sellan, Landry, McGaughey and co-workers[12,50] suggest, at shorter lengths, when more phonons travel ballistically from bath to interface, the apparent resistances decrease. The lower sensitivity of the Kapitza resistance at higher temperatures and the finding that the length at which the Kapitza resistance is essentially length-independent increases at lower temperatures are consistent with the temperature dependence of the phonon population's mean free paths.

Fig. 1(a) shows that the relative lengths of the materials comprising the bicrystal influence the slope of the linear trend; however, the bulk limit, $L \equiv L_{Al} + L_{GaN} \rightarrow \infty$, of Kapitza resistance should be independent of this parameter by physical reasoning. Given the uncertainty induced by the

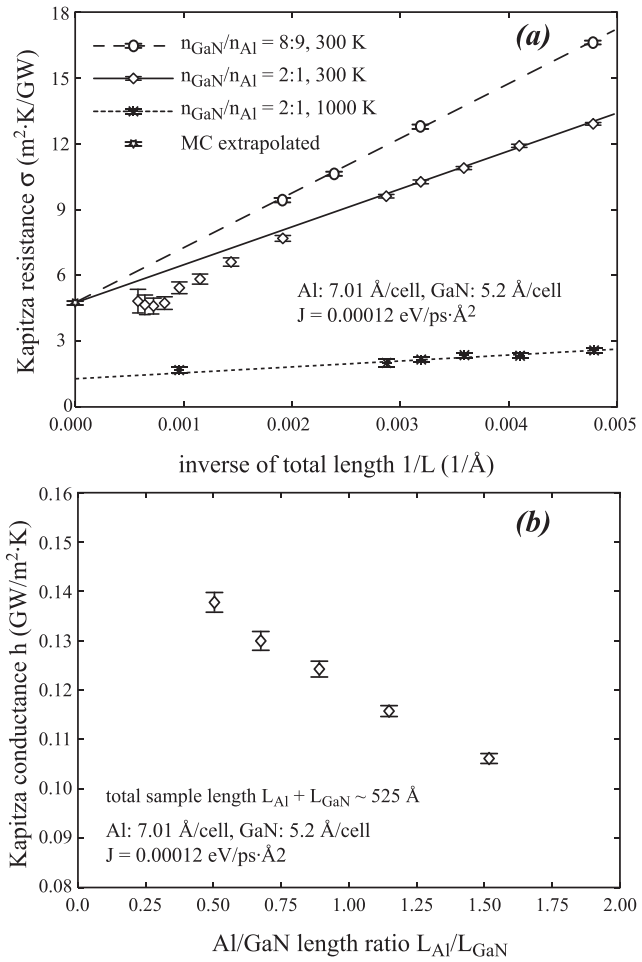

FIG. 1. Size effects in the SW Al:GaN system: (a) the dependence of the Kapiza resistance on total length of the bicrystal at fixed Al:GaN length ratio and (b) the dependence on the length ratio of the two components of the bicrystal for fixed total length. In (a) only data $1/L \geq 0.002\,[1/\text{Å}]$ was used in both 300 K fits to make them comparable. The values for the longest systems are less reliable since the averaging time was reduced to keep the run time feasible. The infinite length error was extrapolated with the Monte Carlo (MC) procedure in Ref. 26.

extrapolation, the infinite length Kapitza resistances at the two ratios studied show remarkable agreement. It is also apparent from Fig. 1(b) that the Kapitza resistance increases with the relative length of the stiffer material (GaN) due to the phonons in the stiffer material having longer mean free paths and therefore more sensitivity to size restrictions than the softer material (Al).

Similar trends in Kapitza resistance *vs.* inverse length are seen in Fig. 2(a) for the simpler LJ system with an acoustic mismatch at 11 K and 31 K (14% and 40% of melt). It is also clear that at higher temperatures the Kapitza resistance is independent of domain size whereas conductivity (Fig. 2(b)) is still sensitive to L. This suggests that the spectra of phonons contributing to Kapitza conductance is different than the spectra of phonons contributing to thermal conductivity, in which only shorter mean-free-path phonons contribute significantly to interface conductance.

Lastly, the effects of electron mediated heat transport and e-ph coupling were simulated with a TTM coupled to the Al lattice of the Al:GaN system. Fig. 3 compares the electronic contributions to Kapitza resistance within the framework of the MD+TTM model at 300 K and 1000 K.

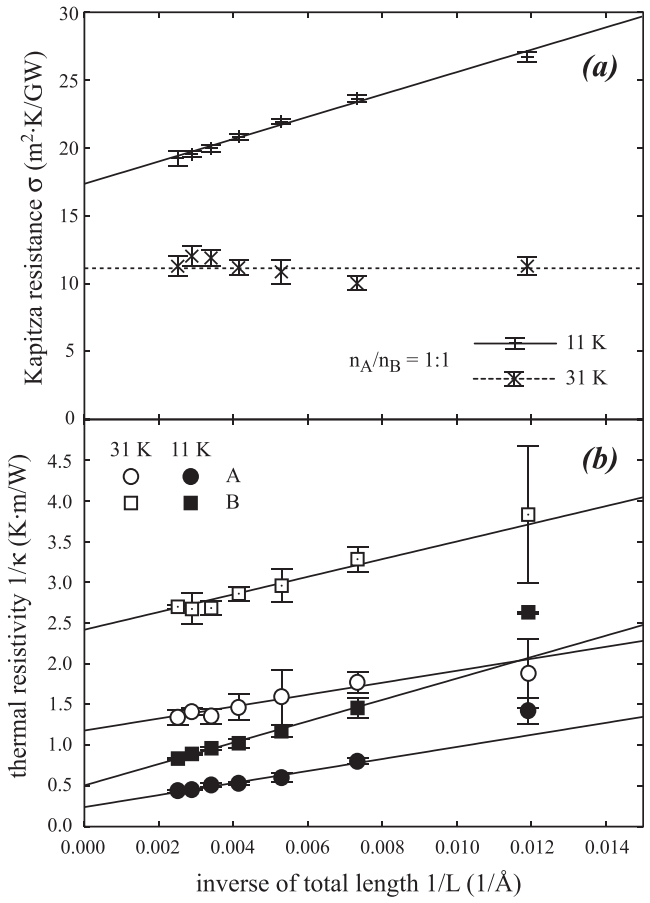

FIG. 2. Kapitza resistance (a) and component resistivities (b) as a function of inverse of system length for the LJ bicrystal, where only the atomic mass differs. The mass of the B component of the bicrystal is 3 times the mass of A, which is nominally the mass of Ar.

The electronic contributions to Al heat conduction become more important at higher temperatures, where the intrinsic phononic thermal conductivity of the Al side is lower. However, since the temperature change across the Al is already quite small with respect to the jump across the interface, the enhanced conductivity simulated with the TTM has a negligible effect on the interface resistance. At both 300 K

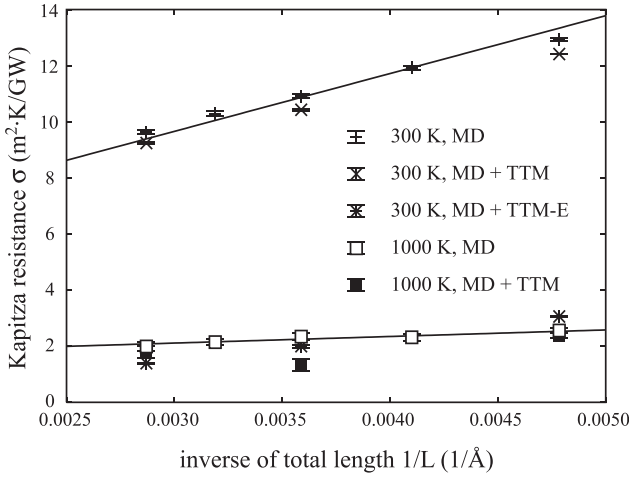

FIG. 3. Al:GaN resistances as a function of total length at 300 K and 1000 K for different two temperature coupling (none: "MD," e-ph coupling in Al only: "MD+TTM," e-ph coupling in Al + 1 unit cell overlap with GaN: "MD+TTM-E").

and 1000 K, when the TTM grid is only on the Al part of the bicrystal, no significant enhancement in Kapitza resistance is observed, but there is a slight systematic decrease in resistance; however, when the TTM grid extends one unit cell into the GaN part of the bicrystal Kapitza conductance is dramatically enhanced. Considering our thermoreflectance measurements of Al:GaN interfaces,[51] $\sigma \approx 10\,m^2\,K/GW$, it is unrealistic to assume electrons are coupling directly to the GaN phonons in this way.

In conclusion, we used large-scale MD simulations of SW Al:GaN and LJ systems to study the dependence of thermal boundary resistance σ on a variety of parameters. The highly converged simulations lead to the following conclusions: (a) σ is independent of the cross-section area under lateral periodic boundary conditions; (b) σ is linearly proportional to inverse of system length, at least in certain regimes, as shown in Figs. 1(a) and 2(a), similar to the Matthiessen rule[50] for thermal conductivity of interface-free materials; (c) the ratio of the lengths of the two components of the bicrystal affects the finite-size interface resistance but not the bulk limit, as in Fig. 1(a); (d) σ becomes length independent at higher temperatures (see Figs. 1(a) and 2(a)) unlike the crystal resistivities, implying that σ is dominated by the contributions of short-wavelength phonons; (e) the apparent increased conductivity due to electron-mediated transport in the metal constituent of a metal-semiconductor contact has little effect on the interface conductance, assuming only phonon-phonon coupling across the interface, as in Fig. 3. If strong e-ph coupling across the interface is assumed, an unreasonably large conductance results. Since these trends where found in both the SW and LJ systems despite different potentials and aspect ratios, we conjecture that these findings are universal.

Whether these trends truly hold up in the bulk limit is currently a matter that must be left to experiments. Also, whether the results are dependent on the interface jump being large relative to the temperature change across each of the materials, scaling with L_A/κ_A and L_B/κ_B *vs.* σ as suggested by Eq. (1), is also left to future work.

The discovery of a scaling rule for interfacial resistance may have important implications. It can provide guidelines for the design of real devices at applicable length-scales and allow MD results obtained on the order of nm to be extrapolated to the infinite system length limit, as is commonly done with the thermal conductivity.[12,26–28,35,47–49] The fact that both thermal resistivity and Kapitza resistance satisfy the same proportionality to inverse total length suggests similar scattering by the heat source/sink and the interfaces between different materials. As our simulations involve both types of interfaces, the scaling rule also confirms the primary assumption of Matthiessen rule, i.e., the scattering sources are essentially additive. The fact that the interface resistance is relatively size independent at higher temperatures may also have important technological implications. Lastly, creating metal-semiconductor interfaces with strong electron-phonon coupling across the interface, if possible, would result in dramatic increases in conductance.

Sandia National Laboratories is a multi-program laboratory managed and operated by Sandia Corporation, a wholly owned subsidiary of Lockheed Martin Corporation, for the U.S. Department of Energy's National Nuclear Security Administration under Contract No. DE-AC04-94AL85000.

[1]P. L. Kapitza, J. Phys. (USSR) **4**, 181 (1941).
[2]E. T. Swartz and R. O. Pohl, Rev. Mod. Phys. **61**, 605 (1989).
[3]P. E. Hopkins, L. M. Phinney, J. R. Serrano, and T. E. Beechem, Phys. Rev. B **82**, 85307 (2010).
[4]D. G. Cahill, W. K. Ford, K. E. Goodson, G. D. Mahan, A. Majumdar, H. J. Maris, R. Merlin, and S. R. Phillpot, J. Appl. Phys. **93**, 793 (2003).
[5]H.-K. Lyeo and D. G. Cahill, Phys. Rev. B **73**, 144301 (2006).
[6]P. M. Norris and P. E. Hopkins, J. Heat Transfer **131**, 43207 (2009).
[7]G. D. Mahan and L. M. Woods, Phys. Rev. Lett. **80**, 4016 (1998).
[8]L. W. da Silva and M. Kaviany, Int. J. Heat Mass Transfer **47**, 2417 (2004).
[9]T. Westover, R. Jones, J. Y. Huang, G. Wang, E. Lai, and A. A. Talin, Nano Lett. **9**, 257 (2009).
[10]P. K. Schelling, S. R. Phillpot, and P. Keblinski, Appl. Phys. Lett. **80**, 2484 (2002).
[11]Y. K. Koh, Y. Cao, D. G. Cahill, and D. Jena, Adv. Funct. Mater. **19**, 610 (2009).
[12]D. P. Sellan, E. S. Landry, J. E. Turney, A. J. H. McGaughey, and C. H. Amon, Phys. Rev. B **81**, 214305 (2010).
[13]E. S. Landry and A. J. H. McGaughey, Phys. Rev. B **80**, 165304 (2009).
[14]M. Hu, P. Keblinski, and P. K. Schelling, Phys. Rev. B **79**, 104305 (2009).
[15]P. K. Schelling, S. R. Phillpot, and P. Keblinski, J. Appl. Phys. **95**, 6082 (2004).
[16]Z.-Y. Ong and E. Pop, Phys. Rev. B **81**, 155408 (2010).
[17]S. Shin, M. Kaviany, T. Desai, and R. Bonner, Phys. Rev. B **82**, 81302R (2010).
[18]R. J. Stevens, L. V. Zhigilei, and P. M. Norris, Int. J. Heat Mass Transfer **50**, 3977 (2007).
[19]R. J. Stevens, P. M. Norris, and L. V. Zhigilei, Proc. IMECE04 **2004**, 60334.
[20]W. J. Evans, M. Shen, and P. Keblinski, Appl. Phys. Lett. **100**, 261908 (2012).
[21]C. F. Carlborg, J. Shiomi, and S. Maruyama, Phys. Rev. B **78**, 205406 (2008).
[22]S. Merabia and K. Termentzidis, Phys. Rev. B **86**, 094303 (2012).
[23]A. S. Henry and G. Chen, J. Comput. Theor. Nanosci. **5**, 141 (2008).
[24]G. Chen, *Nanoscale Energy Transport and Conversion* (Oxford University Press, Oxford, UK, 2005).
[25]Y. Wang, X. Ruan, and A. Roy, Phys. Rev. B **85**, 205311 (2012).
[26]X. W. Zhou, S. Aubry, R. E. Jones, A. Greenstein, and P. K. Schelling, Phys. Rev. B **79**, 115201 (2009).
[27]X. W. Zhou, R. E. Jones, and S. Aubry, Phys. Rev. B **81**, 73304 (2010).
[28]X. W. Zhou, R. E. Jones, and S. Aubry, Phys. Rev. B **81**, 155321 (2010).
[29]F. H. Stillinger and T. A. Weber, Phys. Rev. B **31**, 5262 (1985).
[30]A. Béré and A. Serra, Phys. Rev. B **65**, 205323 (2002).
[31]A. Béré and A. Serra, Philos. Mag. **86**, 2159 (2006).
[32]X. W. Zhou, R. E. Jones, C. J. Kimmer, J. C. Duda, and P. E. Hopkins, Phys. Rev. B **87**, 094303 (2013).
[33]J. C. Duda, T. S. English, E. S. Piekos, T. E. Beechem, T. W. Kenny, and P. E. Hopkins, J. Appl. Phys. **112**, 073519 (2012).
[34]D. V. Matyushov and R. Schmid, J. Chem. Phys. **104**, 8627 (1996).
[35]P. K. Schelling, S. R. Phillpot, and P. Keblinski, Phys. Rev. B **65**, 144306 (2002).
[36]J. C. Duda, C. J. Kimmer, W. A. Soffa, X. W. Zhou, R. E. Jones, and P. E. Hopkins, J. Appl. Phys. **112**, 093515 (2012).
[37]T. Ikeshoji and B. Hafskjold, Mol. Phys. **81**, 251 (1994).
[38]P. Jund and R. Jullien, Phys. Rev. B **59**, 13707 (1999).
[39]D. S. Ivanov and L. V. Zhigilei, Phys. Rev. B **68**, 064114 (2003).
[40]L. Koci, E. M. Bringa, D. S. Ivanov, J. Hawreliak, J. McNaney, A. Higginbotham, L. V. Zhigilei, A. B. Belonoshko, B. Remington, and R. Ahuja, Phys. Rev. B **74**, 012101 (2006).
[41]M. I. Kaganov, I. M. Lifshits, and L. V. Tanatarov, Zh. Eksp. Teor. Fiz. **31**, 232 (1956).
[42]R. E. Jones, J. A. Templeton, G. J. Wagner, D. Olmsted, and N. A. Modine, Int. J. Numer. Methods Eng. **83**, 940 (2010).
[43]A. Majumdar and P. Reddy, Appl. Phys. Lett. **84**, 4768 (2004).

[44]G. D. Mahan, Phys. Rev. B **79**, 075408 (2009).
[45]Z. Lin, L. V. Zhigilei, and V. Celli, Phys. Rev. B **77**, 075133 (2008).
[46]T. S. English, J. C. Duda, J. L. Smoyer, D. A. Jordan, P. M. Norris, and L. V. Zhigilei, Phys. Rev. B **85**, 035438 (2012).
[47]X. Yang, A. C. To, and R. Tian, Nanotechnology **21**, 155704 (2010).
[48]X. W. Zhou and R. E. Jones, J. Phys.: Condensed Matt. **24**, 325804 (2012).
[49]Y. G. Yoon, R. Car, D. J. Srolovitz, and S. Scandolo, Phys. Rev. B **70**, 12302 (2004).
[50]E. S. Landry, M. I. Hussein, and A. J. H. McGaughey, Phys. Rev. B **77**, 184302 (2008).
[51]J. C. Duda, R. Cheato, B. M. Foley, C. Constantin, C.-Y. P. Yang, R. Jones, and P. E. Hopkins, "Thermal conductance across metal:GaN interfaces" (unpublished).